The Effect of Mechano-enzymatic Treatment on the Characteristics of Cellulose Nanofiber Obtained from Kenaf (*Hibiscus cannabinus* L.) Bark

Koranat Narkpiban,[a] Chularat Sakdaronnarong,[b] Thidarat Nimchua,[c] Phitsanu Pinmanee,[c] Paweena Thongkred,[c] and Thitivara Poonsawat [d,*]

Cellulose nanofiber (CNF) was successfully isolated from kenaf bark by microfluidization at 20,000 psi for 40 passes. The combination of hydrothermal process and xylanase treatment prior to CNF isolation led to effective cellulose purification. The fiber used for enzymatic pretreatment for CNF isolation had an 85.9% whiteness index and 85.1% cellulose content. The crystallinity of the cellulose extracted from the kenaf bark continued to increase with successive treatments, as indicated by X-ray diffraction analysis. In addition, the enzyme-treated fiber showed increased thermal stability, as shown by thermogravimetric analysis. After CNF isolation, morphological characterization of the CNF was performed *via* field emission-scanning electron microscopy and transmission electron microscopy. The CNF had an average diameter that ranged from 5 to 10 nm and no undesired elemental contamination, as evidenced by energy dispersive X-ray spectroscopy. The mechano-enzymatic treatments used in this work to obtain CNF were judged to be a promising technique for the fabrication of biomedical and other high-value materials.

Keywords: Cellulose nanofiber; Hydrothermal treatment; Kenaf; Mechano-enzymatic; Microfluidization; Xylanase

Contact information: a: Bioproduct Science, Department of Science, Faculty of Liberal Art and Science, Kasetsart University, KamphaengSaen, NakhonPathom 73140, Thailand; b: Department of Chemical Engineering, Faculty of Engineering, Mahidol University, 25/25 Phutthamonthon 4 Road, Salaya, Phutthamonthon, NakornPathom 73170, Thailand; c: Enzyme Technology Laboratory, Microbial Biotechnology and Biochemicals Research Unit, National Center for Genetic Engineering and Biotechnology (BIOTEC), 113 Thailand Science Park, Phahonyothin Road, KhlongNueng, KhlongLuang, PathumThani 12120, Thailand; d: Department of Botany, Faculty of Liberal Arts and Science, Kasetsart University, Kamphaeng Saen, Nakhon Pathom 73140, Thailand;
** Corresponding author: faastrp@ku.ac.th*

INTRODUCTION

Currently, research on the development of biodegradable nanomaterials from renewable resources is a challenging task because of the growing demand in the biocomposites (Alemdar and Sain 2008; Bandyopadhyay-Ghosh *et al*. 2010), biomedical materials (Lin and Dufresne 2014; Liang *et al*. 2017), and electronic substrates industries (Sabo *et al*. 2016). Nanocellulose is obtained from the cellulose from plants or bacteria (Bandyopadhyay-Ghosh *et al*. 2010; Lin and Dufresne 2014) and shows several superior properties, such as high surface area, unique optical properties, nanoscale dimensions, high crystallinity, and high strength and stiffness, together with the renewability and biocompatibility of cellulose (Oun and Rhim 2016). Nanocellulose is commonly prepared by subjecting the plant lignocellulosic materials to treatment and delignification processes

using single or combined mechanical, chemical, and enzymatic methods to disrupt cellulose-hemicellulose-lignin complexes (Agbor *et al*. 2011).

In general, nanocellulose from plants can be separated into two categories: cellulose nanofiber (CNF) and cellulose nanocrystal (CNC). The CNF has a rope-like shape and consists of long, flexible nanostrings 5 to 60 nm in diameter with a length on the micrometer scale, formed by alternating crystalline and amorphous domains (Zhao *et al*. 2013; Saelee *et al*. 2016). The CNC consists of needlelike cellulose crystals 10 to 20 nm in width and several hundred nanometers in length and has limited flexibility compared to CNF because of its high crystallinity (Rahimi Kord Sofla *et al*. 2016). The CNCs are often generated *via* intense acid hydrolysis, while CNFs can be generated by various mechanical processes (Martelli-Tosi *et al*. 2016), such as refining or high-shear homogenization (Kaushik and Singh 2011), high-pressure homogenization (Li *et al*. 2014), microfluidization (Liu *et al*. 2017), ultrafine grinding (Hassan *et al*. 2014), cryocrushing (Alemdar and Sain 2008), and ultrasonication (Khawas and Deka 2016; Xie *et al*. 2016). These mechanical techniques provide sufficient shear forces to separate cellulose fibers along the longitudinal axis and assist in separating microfibrillated cellulose from plant fibers (Hassan *et al*. 2014). A major barrier that must be overcome for the successful commercialization of CNF is the time and energy consumption, as high energy is required for the mechanical disintegration of the starting cellulose macrofibers into nanofibers (Xie *et al*. 2016). Treatment processes, such as hydrothermal and enzymatic hydrolysis, need to be performed prior to the mechanical processes to lower the process costs, minimize the operating time, and reduce the environmental impacts of the energy use.

Hydrothermal treatment (HTP) is a physicochemical process and is known as the most effective treatment method in terms of operational simplicity, with mild reaction conditions, low costs, and environmental friendliness (Gan *et al*. 2015). The HTP can break down lignocellulosic structural components (lignin, cellulose, pectin, and hemicellulose) to open up the fiber structure by using liquid water under elevated temperature and pressure (Patel *et al*. 2016), thus enabling accessibility to the polysaccharide components of the raw lignocellulose. In addition, this treatment helps to partially solubilize the hemicelluloses and separate the lignin structure, resulting in a larger crystalline region and a higher specific surface area (Xiao *et al*. 2011; Ma *et al*. 2013). Generally, the HTP is influenced by several factors, including temperature, time, and solid-to-liquor ratio. Among these factors, temperature is considered the most important parameter in the process due to the chemical compositions of the fiber that are degraded at different temperatures. The temperature during processing can vary in a wide range, between 100 °C and 250 °C (Fan *et al*. 2016). During HTP, the acetyl ester bonds of xylan in hemicellulose are hydrolyzed to yield acetic acid as a byproduct, which could also serve as a catalyst to encourage hemicellulose degradation and acquisition. Consequently, the oligosaccharides in the solution are further hydrolyzed to sugar monomers as products of degradation (Agbor *et al*. 2011; Xiao *et al*. 2011). Lignin depolymerization and solubilization partially occur during the HTP, but the complete delignification of lignocellulosic material is not possible because of the recondensation of soluble components originating from lignin (Alvira *et al*. 2010). Hence, the remaining fraction of lignin in the cellulose residue obtained from the HTP process must be removed by the process of chemical bleaching, which conventionally employs a large amount of chlorine and chlorine-based chemicals. However, the use of such chemicals liberates several toxic materials and polluting products that contaminate the bleaching effluent, including absorbable organic halides (AOX) (Gangwar *et al*. 2016; Pei *et al*. 2016).

A recent alternative technique with greater prospects for long-term consequences is xylanase treatment; this technique has been used before the bleaching process to decrease the use of chemicals (Gangwar *et al*. 2016; Saelee *et al*. 2016). The beneficial effect of xylanase during the delignification process is the selective hydrolysis of xylan reprecipitated on the fiber surface, which improves the permeability of the fiber to the bleaching chemicals (Roncero *et al*. 2005; Gangwar *et al*. 2016). Moreover, xylanase treatment increases the extractability of the chromophores associated with lignin-carbohydrate complexes (LCCs) and the hydrophobic materials from the fibers, as indicated by an increase in fiber brightness (Shatalov and Pereira 2009; Gangwar *et al*. 2016). The application of xylanases as bleach boosting agents has been known to save chemical costs without interfering with the existing process and also allows for a remarkable reduction in the bleaching chemicals and minimizes environmental impact (Gangwar *et al*. 2016)

Currently, the utilization of annual plants and agricultural residues, including cotton, banana, flax, hemp, sisal, jute, and kenaf for the production of CNF has been a topic of intense research in various studies (Marrakchi *et al*. 2011). Kenaf (*Hibiscus cannabinus* L.) is one of the annual plants that is considered a feasible source of CNF with economic and ecological benefits.

Kenaf consists of two types of fibers: the core and the bast fibers. The core fiber is the inner layer of a fiber (70% of dry weight), while the bast fiber refers to the outer layer of the plant fiber (30% of dry weight). Bast fiber has been reported to have excellent mechanical and physical characteristics for use in generating CNF (Jonoobi *et al*. 2009; Karimi *et al*. 2014; Sulaiman *et al*. 2015). However, although there are many treatment methods for the separation of CNF from kenaf, few are based on economic and environmental considerations. Thus, many studies have focused on using a combination of enzymatic and mechanical treatment methods to reduce both energy and chemical use during CNF isolation (Siddiqui *et al*. 2010; Janardhnan and Sain 2011; Kalia *et al*. 2013; Hassan *et al*. 2014; Saelee *et al*. 2016).

For ‘green’ CNF production, microfluidization is one of the mechanical methods widely used to produce CNF and involves the cellulosic materials through an intensifier pump that generates forces of up to 40,000 psi (276 MPa), followed by an interaction chamber that defibrillates the fibers by shear forces at a constant shear rate (Saelee *et al*. 2016; Liu *et al*. 2017). This repeatable process results in tiny particles with a uniform distribution. However, using only microfluidization has a negative effect, as it decreases the crystallinity and damages the fiber structure, and energy consumption increases greatly with increasing treatment time (Henriksson *et al*. 2007). In addition, CNF produced from microfluidization alone tends to aggregate and cause extensive clogging, which may be the major limitation in the application of CNF (Abdul Khalil *et al*. 2016). To address this issue, enzymatic treatment of lignocellulosic materials needs to be optimally combined with microfluidization to decrease flocculation and clogging and consequently lower the energy consumption of the CNF isolation process. Consequently, this work aims to find an ecofriendly alternative method for the isolation of nanometer-sized single fibers of cellulose, or CNF, from kenaf bark. To the best of the authors’ knowledge, this work is the first to use kenaf bark to isolate CNF *via* enzymatic treatment and mechanical processes to reduce the amount of chemical consumption involved.

EXPERIMENTAL

Materials

Kenaf (*Hibiscus cannabinus*, var Khon-Kaen 60) bark was obtained from the Khon-Kaen Agronomy Research Center, Khon-Kaen, Thailand. Kenaf bark was milled into particle sizes between 125 to 180 μm. The xylanase from *Aspergillus* sp. was used in the enzymatic treatment and was prepared at the Enzyme Technology Laboratory, National Center for Genetic Engineering and Biotechnology (BIOTEC) in Pathum Thani, Thailand. The chemical agents used in the bleaching process, including sodium chlorite ($NaClO_2$) and glacial acetic acid, were supplied by Merck (Darmstadt, Germany) and were of analytical grade.

Methods

Xylanase concentration on hydrolysis of the kenaf bark

To determine the effect of xylanase on fiber degradation, bast tissue from the stem of kenaf was manually separated and milled into 125 to 180 μm lengths. Approximately 0.15 g dry weight (DW) of bast section was transferred to a 5-mL centrifuge tube containing 1.5 mL of 50 mM sodium acetate buffer at pH 5.5. The mixture was incubated overnight at 30 °C under agitation (220 rpm). After an equilibration period, xylanase was added to reach activities of 20, 50, 500, and 5000 U/g fiber. One unit (U) of enzyme activity was the amount of xylanase activity necessary to release 1 μmole of xylose equivalent per min at 50 °C. The reaction mixture was incubated at 50 °C under agitation (220 rpm). The samples were taken after 24 h of incubation. Subsequently, the mixed liquid was centrifuged at 12,000 rpm for 10 min and filtered through a syringe filter (13 mm NYL 0.2 μm, Xiboshi, Tianjin Fuji Science & Technology Co., Ltd., Tianjin, China) before analysis of the total reducing sugar by the dinitrosalicylic acid (DNS) method (Miller 1959). All experiments were conducted in triplicate, and their results are given as the mean and standard deviation.

Hydrothermal treatment of kenaf bark

The hydrothermal treatment of kenaf bark was performed in a high-pressure reactor (Parr 4848 reactor controller, Parr Instrument Company, Moline, IL, USA) at 160 °C for 40 min with a fixed fiber to liquor ratio of 1:10. Subsequently, the reactor was cooled immediately, and the hydrothermally pretreated kenaf fiber was obtained *via* filtration, then oven-dried overnight, and stored for later enzymatic treatment.

Enzymatic treatment of hydrothermally pretreated kenaf bark

The hydrothermally pretreated kenaf fibers were mixed with a xylanase concentration of 5000 U/g fiber at pH 5.5 using a fiber-liquid ratio of 1:10, where the control was the kenaf fiber and buffer (NaAc buffer). The reaction mixture was further incubated at 50 °C with constant agitation (220 rpm) for 24 h. After completion of the enzymatic treatment, the sample fibers were washed well with deionized water and dried at 70 °C for 24 h.

Bleaching process

The bleaching process was adapted from Saelee *et al*. (2016). Briefly, a mixture of hydrothermally pretreated fibers and bleaching solution ($NaClO_2$ at 2% w/v, adjusted to pH 3.0 with acetic acid) was added to 250-mL Erlenmeyer flasks with a fiber-to-liquid

ratio of 1:10. The bleaching process took place at 70 °C in a water bath. A fresh bleaching solution was replaced hourly at the same loading ratio, this was done 4 times. After 4 h of bleaching, the bleached fibers were washed with deionized water until the pH became neutral. Finally, the solid residue was dried in a hot air oven at 60 °C for 24 h.

Preparation of CNF from bleached kenaf fiber

The CNF was produced from kenaf fiber after sequential hydrothermal treatment, enzymatic treatment, and bleaching (HT-KF-x5000-B, Table 1) using a microfluidizer (Microfluidizer M-110P; Microfluidics Corp., Westwood, MA, USA). Diluted suspensions (0.2% w/v) of the HT-KF-x5000-B kenaf sample were prepared and soaked in distilled water for 24 h. The suspensions were processed in the microfluidizer with an 87-μm sized at 20,000 psi for 40 passes. Finally, the CNF was collected *via* centrifugation at 5,000 rpm for 15 min and kept in aqueous solution in the refrigerator until use. The list of fiber sample acronyms is given in Table 1.

Table 1. List of Fiber Acronyms at Different Stages of Treatment in the CNF Isolation Process

Sample	Conditions
KB	Kenaf bark
HT-KF	Hydrothermally pretreated kenaf fibers
HT-KF-NaAc buffer	Hydrothermally pretreated kenaf fibers + Sodium acetate buffer
HT-KF-x5000	Hydrothermally pretreated kenaf fibers + Xylanase concentration of 5,000 U/g fiber
HT-KF-NaAc buffer-B	Hydrothermally pretreated kenaf fibers + Sodium acetate buffer + Bleaching
HT-KF-x5000-B	Hydrothermally pretreated kenaf fibers + Xylanase concentration of 5,000 U/g fiber + Bleaching
CNF	Hydrothermally pretreated kenaf fibers + Xylanase concentration of 5,000 U/g fiber + Bleaching + Microfluidization

Characterization

Chemical composition of kenaf fiber

The chemical compositions of raw kenaf bark and the fibers obtained after each process were analyzed according to the method developed by Van Soest (1963). The amounts of neutral detergent fiber (NDF), acid detergent fiber (ADF), and acid detergent lignin (ADL) were determined *via* a fiber analyzer (ANKOM A200; ANKOM Technology, Macedon, NY, USA) using a gravimetric analysis technique. Each sample was measured in triplicate. The hemicellulose, cellulose, and lignin contents were calculated as follows according to Eqs. 1 through 3:

$$\text{Hemicellulose} = \text{NDF} - \text{ADF} \quad (1)$$

$$\text{Cellulose} = \text{ADF} - \text{ADL} \quad (2)$$

$$\text{Lignin} = \text{ADL} \quad (3)$$

Color analysis of kenaf fiber

The changes in fiber color were evaluated by a spectrophotometer (Datacolor 650™; Datacolor, Lawrenceville, NJ, USA). A white standard plate was utilized to calibrate the device prior to color measurement (L = 96.37, a = -0.1, and b = 1.33). The

color values are shown in three coordinate dimensions: L^* lightness (0 = black, 100 = white), a^* redness/greenness (-a^* = green; +a^* = red), and b^* yellowness/blueness (-b^* = blue; +b^* = yellow), including the total color difference (ΔE) value. Each sample was measured in triplicate. The whiteness index (WI) value was computed based on Eq. 4 according to Ghanbarzadeh *et al*. (2010).

$$WI = 100 - [(100 - L)^2 + a^2 + b^2]^{0.5} \quad (4)$$

Field emission-scanning electron microscopy (FE-SEM)

The surface morphology of the kenaf fiber and CNF was investigated using field emission-scanning electron microscopy (Hitachi Schottky FE-SEM: SU5000 with EM wizard, Tokyo, Japan). The specimen was deposited on the electron microscope grids, and FE-SEM was performed at an accelerating voltage of 10 kV for the kenaf fiber and of 5 kV for CNF in low- and high-vacuum modes.

Transmission electron microscopy (TEM)

The CNF morphology was analyzed under a transmission electron microscope (Hitachi model HT7700; Tokyo, Japan) with an accelerating voltage of 80 kV. The CNF suspension was diluted and sonicated for 30 min. A carbon-coated copper grid was attached above the surface of the diluted CNF droplet. Then, the grid was inverted, allowed to contact a drop of 2% (w/v) uranyl acetate solution for 5 min, and then air-dried at room temperature. The CNF diameter was measured using the software Fiji/ImageJ-win64 (National Institutes of Health, version 1.51d, Bethesda, MD, USA). The average diameter and length of the CNF were determined from 150 fibers in the TEM images.

Energy dispersive X-ray spectroscopy (EDS)

The elemental composition of the sample was analyzed using the EDS technique (Model: RTEM, EDAX Inc., Mahwah, NJ, USA) in combination with TEM. The EDS spectrum obtained from the spot profile revealed the elemental distribution in the sample.

Fourier-transform infrared spectroscopy (FTIR)

The spectra of the fibers after processing were obtained using an FTIR spectrometer (Nicolet 6700; Thermo Scientific, Madison, WI, USA). Each sample was blended with KBr powder, and the mixture was compressed to form a disk. The IR spectra of the fiber samples were measured in transmission mode at 4 cm^{-1} resolution with 64 scans in a scan range of 4000 to 400 cm^{-1} with a deuterated triglycine sulfate (DTGS) detector.

X-ray diffraction (XRD)

The XRD patterns of the fibers after each process were obtained by using a high-resolution X-ray diffractometer (PANalytical, X'pert PRO, Almelo, Netherlands). Scattered radiation was detected at a 2θ angle from 5° to 60° at a scanning rate of 0.02°/0.5 s scanning rate. The crystallinity index (CrI) was defined by following the XRD peak height method, where the CrI was computed from the height of the 002 peak (I_{002}) and the height of the minimum (I_{am}) between the 002 and 001 peak according to Eq. 5 (Segal *et al*. 1959),

$$CrI\ (\%) = [(I_{002} - I_{am}) / I_{002}] \times 100 \quad (5)$$

where CrI (%) represents the relative degree of crystallinity, I_{002} is the intensity of both the crystalline and amorphous regions, and I_{am} is the intensity of the amorphous region alone.

Atomic force microscopy (AFM)

The morphology of the CNF after microfluidization was observed by AFM (Asylum, MFP-3D AFM (bio), Oxford Instruments, Santa Barbara, CA, USA) at room temperature. The dilute CNF suspension was dropped onto the surface of an optical glass. Then, the sample was air-dried at room temperature and subsequently analyzed.

Thermogravimetric analysis (TGA)

The thermal stability and decomposition temperature of all samples after treatment were determined using a TGA/851^e/1600 thermogravimetric analyzer (Mettler Toledo, Schwerzenbach, Switzerland). The samples were heated from 27 °C (room temperature) to 500 °C at a heating rate of 10 °C/min in an ambient nitrogen atmosphere.

RESULTS AND DISCUSSION

Effect of Xylanase Concentration on the Hydrolysis of Kenaf Bark

The effect of xylanase concentration on kenaf bark hydrolysis was investigated by monitoring the amount of total reducing sugars released. The hydrolysis of hemicellulose in kenaf bark increased with the concentration of enzyme used for the treatment (Fig. 1).

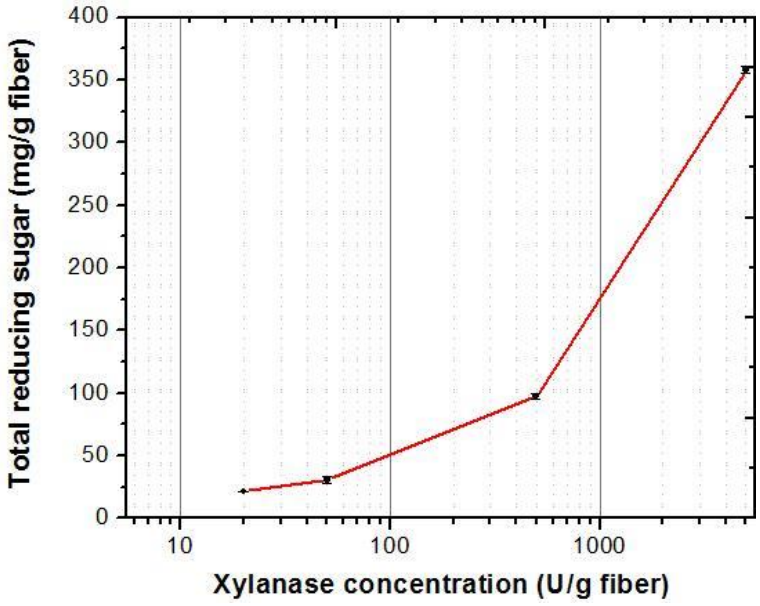

Fig. 1. The effect of xylanase at various concentrations (20, 50, 500, and 5000 U/g biomass) on kenaf bark hydrolysis at 50 °C for 24 h (mean value ± standard deviation are shown)

The amounts of reducing sugars obtained after enzymatic hydrolysis with 20, 50, 500, and 5,000 U/g of xylanase activity at 50 °C and pH 5.5 for 24 h were 23.74, 33.03, 99.59, and 360.01 mg/g fiber, respectively. The enzyme hydrolysis at 5,000 U/g clearly gave a maximum amount of reducing sugars, 3.61-, 10.90-, and 15.16-fold greater than the xylanase treatment at the concentrations of 500, 50, and 20 U/g, respectively. In this

experiment, xylanase was not purified that contained pectinase activity (data not shown). Therefore, the preparation of kenaf fiber by retting process was skipped. Either pectic substance, a main component of middle lamella, or xylose was removed from kenaf bark in this process. Thus, 5,000 U/g of xylanase is considered. As relationship between enzyme concentrations and substrates in terms of catalytic activity, xylanase activity is defined as follows: "One unit (U) of enzyme activity was the amount of xylanase activity necessary to release 1 µmole of xylose equivalent per min at 50 °C." Thus, in 1 hour, 20 U/g of xylanase can liberate 1,200 micromoles of xylose, while 5000 U/g of xylanase can liberate 300,000 micromoles of xylose. Therefore, excess xylan in the sample was suitable for the high enzyme activity of xylanase. The concentration of 5000 U/g. xylanase was selected for further investigation on kenaf fiber peeling after hydrothermal treatment.

Effect of Treatment on the Chemical Composition of Kenaf Fibers

The chemical compositions of the fiber after processing are presented in Fig. 2. The percentages of cellulose, hemicellulose, and lignin in the KB specimens were 57.6%, 22.7%, and 2.87%, respectively. After hydrothermal treatment, the cellulose and lignin contents increased from 57.6% and 2.87% to 69.2% and 6.29%, respectively, whereas the hemicellulose content decreased from 22.7% to 14.7% because the hemicelluloses were hydrolyzed into water-soluble sugars. In addition, pectin and acid-soluble lignin were partially removed from the sample, which facilitated the reduction of acid-insoluble lignin after hydrothermal processing (Zhang *et al*. 2016). After subsequent hydrothermal, xylanase, and bleaching treatments of the kenaf bark, the cellulose content of HT-KF-X5000-B increased from 57.6% to 85.1%, whereas the hemicellulose content declined from 22.7% to 4.05%, and the lignin decreased from 2.87% to 0.15%. The increase in cellulose content was always accompanied by a decrease in the hemicellulose and lignin. This change in chemical composition confirmed that noncellulosic moieties were effectively removed during the treatments.

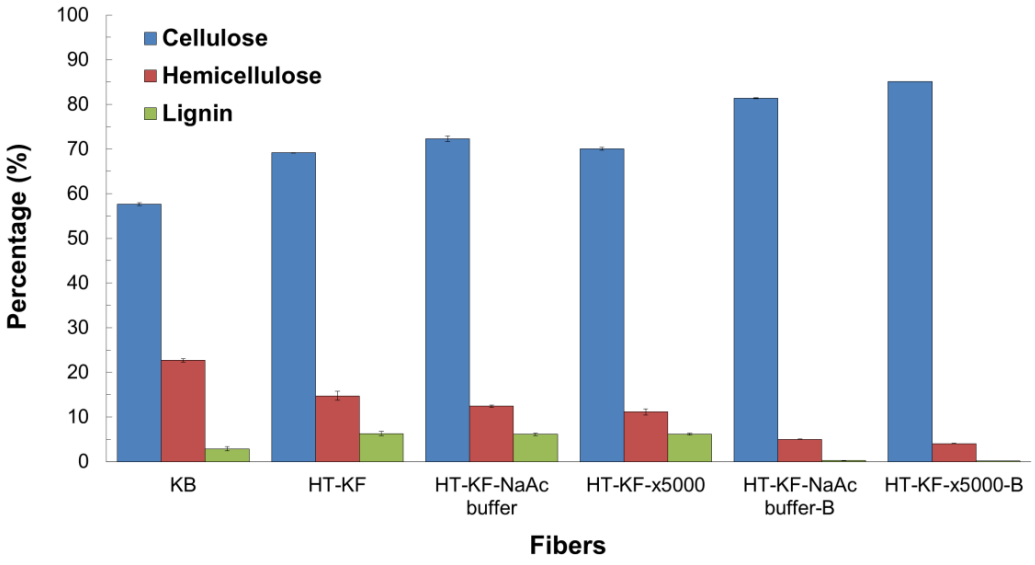

Fig. 2. Chemical compositions (mean value ± standard deviation) of the fiber at different stages of treatment

Effect of Treatment on the Color of Kenaf Fibers

The whiteness index (WI) of the fiber samples after different treatments indicated the color changes after each treatment, and the appearance of the fibers is illustrated in Fig. 3. The native kenaf bark, or KB, (Fig. 3a) was a light brown color, and the WI value was 62.9. After hydrothermal treatment, the HT-KF fiber (Fig. 3b) was a dark brown color, and the WI value decreased to 50.0. The darker color of the KB after hydrothermal treatment was due to changes in the lignin or its removal and/or dislocation during the hydrothermal process, in addition to the recondensation of the solubilized lignin onto the fiber surface. Thus, the amount of residual lignin after hydrothermal treatment increased from the amount of starting lignin in the raw fiber (Kumar *et al*. 2013; Saelee *et al*. 2016). After xylanase treatment, the WI values of the HT-KF-X5000 fibers (Fig. 3d) did not change when compared to the WI values of the HT-KF fibers. Therefore, the hemicellulose dissolution did not affect the whiteness of the fiber. For the control of the xylanase treatment, the HT-KF-NaAc sample (Fig. 3c) had similar WI to the HT-KF sample. After bleaching, the HT-KF-X5000-B fiber (Fig. 3f) was completely white, with a WI of 85.9, due to bleaching agents that either oxidized or reduced the lignin-derived chromophores. The xylanase treatment control, HT-KF-NaAc buffer-B fibers, had a slightly lower WI, 82.15, compared to that of the xylanase-treated fiber, as shown in Fig. 3e. The HT-KF-X5000-B fiber was brighter than the HT-KF-NaAc buffer-B fiber. This indicated that the HT-KF-NaAc buffer-B fiber need more bleaching chemicals than the HT-KF-X5000-B fiber. Consequently, the effects of the xylanase treatment on the kenaf fiber were substantially clearer after the bleaching process.

This result indicated that the xylanase treatment prior to the bleaching processes was effective, as it facilitated an increase in the brightness of the fibers. The reason was that xylanase treatment assisted the bleaching chemical in penetrating the fibers easily for lignin removal, and thus, less of the bleaching chemical was required. These findings were in good agreement with previously reported results regarding the efficiency of xylanase-assisted treatment for the isolation of cellulose nanofibrils from sugarcane bagasse (Saelee *et al*. 2016).

In general, color is an important key of cellulose fiber because it is used by the customer in many applications. According to the results of color changes, the HT160-KF-X5000-B fiber generated satisfactory color. Thus, the HT160-KF-X5000-B fiber was selected for CNF isolation.

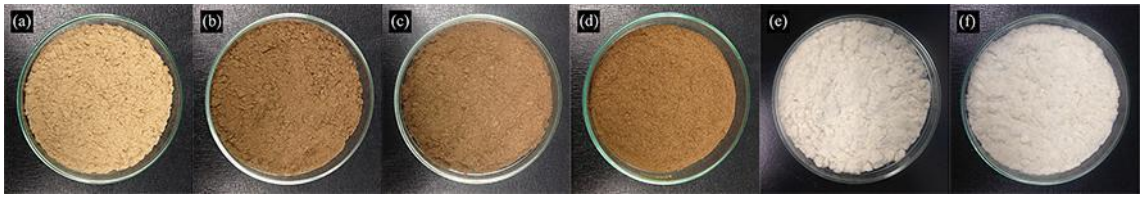

Fig. 3. Images of (a) KB, (b) HT-KF, (c) HT-KF-NaAc buffer, (d) HT-KF-x5000, (e) HT-KF-NaAc buffer-B, and (f) HT-KF-x5000-B

Electron Microscopy Analyses (FE-SEM, TEM, and AFM)

Figure 4 (4a to 4f) shows the fiber surface at each stage of CNF isolation. The FE-SEM image of the KB fiber surface (Fig. 4a) shows the materials covering the fiber bundles that link an individual single fiber into the macro structure. Noncellulosic constituents, such as lignin and hemicellulose, as well as other impurities, such as wax and pectin, were

also observed (Karimi *et al*. 2014; Sulaiman *et al*. 2015). After hydrothermal treatment at 160 °C, the surface topography of the HT-KF (Fig. 4b) was less smooth because the noncellulosic constituents were removed. This was consistent with the chemical composition of the hydrothermally-treated fiber (Fig. 2). The FE-SEM images showed that the HT-KF-x5000 specimens (Fig. 6d) were less aggregated than the HT-KF-NaAc buffer specimens (Fig. 4c). Therefore, the xylanase treatment facilitated the better separation of the fiber from the bundles. After bleaching, the HT-KF-x5000-B specimens (Fig. 4f) were more disrupted than the HT-KF-NaAc buffer-B specimens (Fig. 4e). This result implied that the enzyme treatment and bleaching process substantially affected the microstructure of the kenaf fibers, which may not be detected by low-magnification imaging and chemical composition analysis. However, the efficiency of the enzyme treatment may change the internal microstructure of the crystallinity of cellulose and the matrix without changing the major components. Thus, the enzyme-treated samples allowed for greater penetration than the untreated samples. Figures 4g and 4h show the FE-SEM micrographs of CNF from the HT-KF-x5000-B suspension after microfluidization and after freeze-drying, respectively. A complete disintegration of cellulose fiber was found after microfluidization.

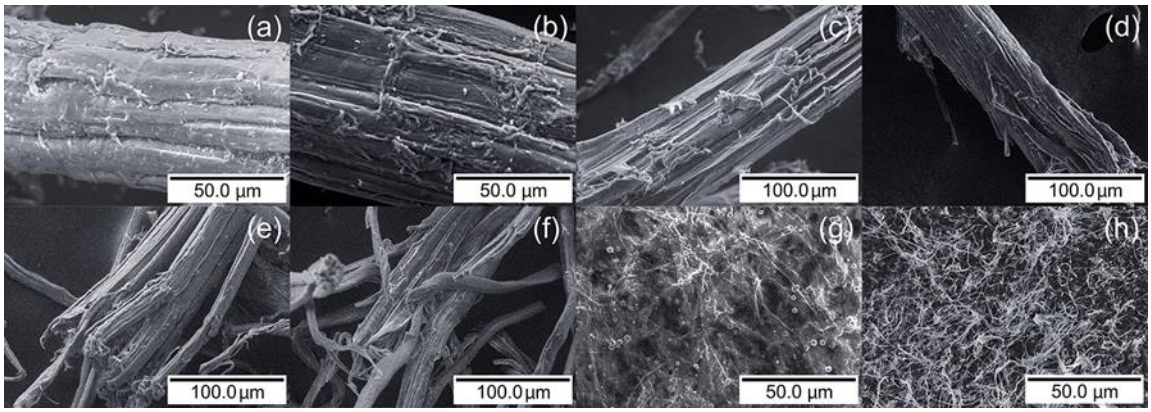

Fig. 4. FE-SEM images of (a) KB, (b) HT-KF, (c) HT-KF-NaAc buffer, (d) HT-KF-x5000, (e) HT-KF-NaAc buffer-B, (f) HT-KF-x5000-B, (g) CNF suspension after microfluidization, and (h) CNF after freeze-drying

As shown in Fig. 5, the microfluidization process led to the formation of nanofibers, as indicated by the nanodimensional scale of the objects observed in the TEM and AFM images. The TEM images of CNFs at different scales are illustrated in Fig. 5a and 5b. These images revealed CNF filaments form a web-like structure. The diameter distribution of CNF is shown in Fig. 5c. More than 80% of CNFs are 5 to 15 nm in diameter, and their length was several micrometers. Moreover, the nanometer dimensions of CNF were also supported by AFM imaging (Fig. 5d). Therefore, these results indicated that the CNF obtained after microfluidization at 20,000 psi for 40 passes was completely isolated on a nanometer scale.

EDS Analysis

The EDS spectrum of CNF shows the energy levels of carbon and oxygen in the sample, as shown in Fig. 6. The amount of carbon was higher than the amount of oxygen: the composition was 71.09% carbon and 28.91% oxygen. The chemicals applied in several treatment steps, especially sulfur, sodium, and chlorine, used in the xylanase treatment and bleaching process, were not found in the final CNF.

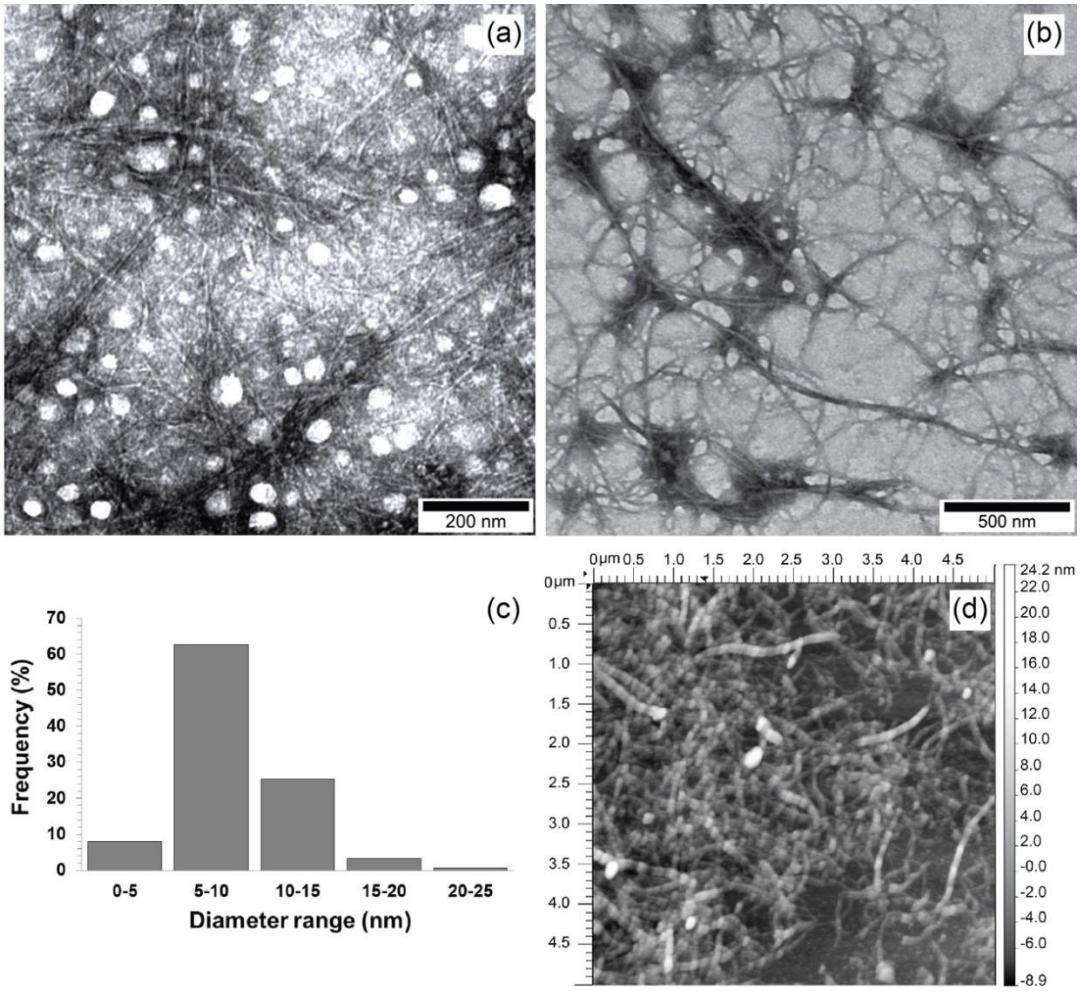

Fig. 5. The morphology of CNF: (a and b) TEM images at different magnifications, (c) diameter distribution, and (d) AFM image of CNF

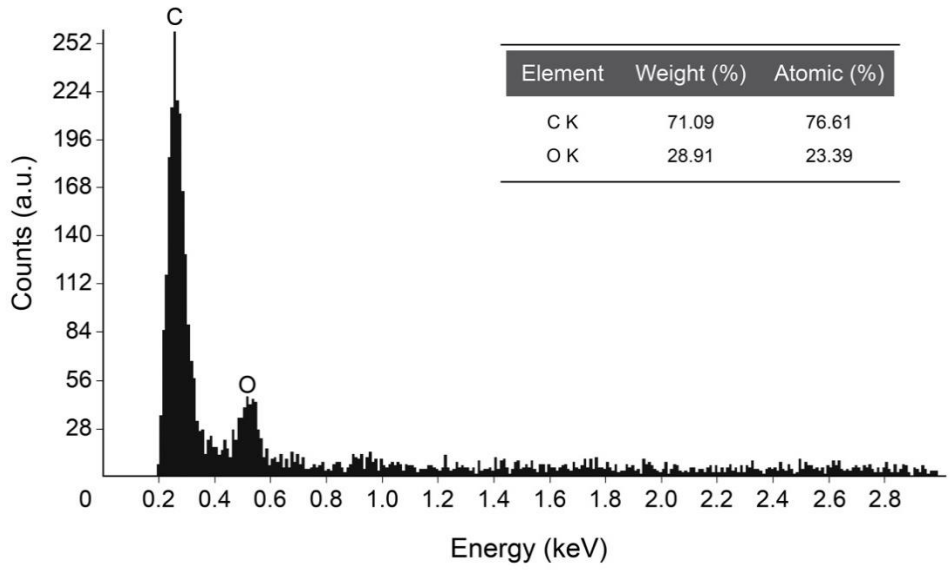

Element	Weight (%)	Atomic (%)
C K	71.09	76.61
O K	28.91	23.39

Fig. 6. EDS spectrum of kenaf CNF

The results were in contrast to those of a previous report, as the chemical residues in the final CNF, such as sulfur and sodium, were present in significant amounts (Rahimi Kord Sofla *et al*. 2016). Based on these results, the CNF-based materials derived from the present work can be concluded as suitable for biomedical applications, because high-purity CNF is required for safe use (Liang *et al*. 2017). Changing the bleaching agent from $NaClO_2$ to H_2O_2 would be interesting to investigate in the future as a means of achieving safer and more environmentally friendly CNF production (Martelli-Tosi *et al*. 2016).

FTIR Spectroscopy Analysis

To analyze the changes in the chemical structure of fiber bundles, fibers, and CNF after various treatments, FTIR spectroscopy was used. Figure 7 shows the FTIR spectra of (a) KB, (b) HT-KF, (c) HT-KF-NaAc buffer, (d) HT-KF-x5000, (e) HT-KF-NaAc buffer-B, (f) HT-KF-x5000-B, and (g) CNF specimens. The absorbance peaks at 3500 to 3200 cm^{-1} found in the spectra of all samples were attributed to the O-H stretching and bending vibrations of the hydrogen-bonded hydroxyl groups, and the absorption in the range of 2900 to 2800 cm^{-1} was assigned to the C-H stretching vibration of the alkyl groups in the aliphatic bonds of cellulose (Karimi *et al*. 2014; Chandra *et al*. 2016; Saelee *et al*. 2016). The peaks located at wavenumber 1640 cm^{-1}, related to the O-H bending vibrations of the adsorbed water in a cellulose fiber structure (Karimi *et al*. 2014), could be found for all samples. The peak at 1600 cm^{-1} was associated with functional groups such as methoxyl-$O-CH_3$, C-O-C, and aromatic C=C (Abraham *et al*. 2013; Chandra *et al*. 2016). This 1600 cm^{-1} peak was absent in the spectrum of bleached fiber and CNF because the lignin content was completely removed after the bleaching process.

The absorbance at 1506 cm^{-1} of the KB, HT-KF, HT-KF- NaAc buffer, and HT-KF-x5000 fiber spectra was associated with the C=C stretching vibration of the aromatic ring of lignin (Xu *et al*. 2015). This characteristic peak at wavenumber 1506 cm^{-1} disappeared completely in the spectra of specimens of bleached fiber (HT-KF-NaAc buffer-B and HT-KF-x5000-B) and CNF; however, it was present in the spectra of the unbleached samples (HT-KF-NaAc buffer and HT-KF-x5000). Moreover, the peak at wavenumber 1460 cm^{-1} corresponded to the C-H bending patterns of the lignin and hemicellulose as well as the C=C vibrations of the aromatic structure in lignin. This peak disappeared from the spectrum of bleached fiber as well as from the spectra of the CNF. It was concluded that the bleaching process removed most of the hemicellulose and lignin from the kenaf fiber and CNF.

For polysaccharide absorption, the absorbance between 1430 to 1420 cm^{-1} and 1380 to 1330 cm^{-1} in all samples was associated with the symmetric bending of CH_2 and C-O bonds in the polysaccharide aromatic ring (Jonoobi *et al*. 2009). Moreover, at 1032 cm^{-1}, the wavenumber peaks of all samples were associated with the C-O, C-C stretching, or C-OH bending of cellulose and hemicellulose (Xu *et al*. 2015). This peak was completely absent from the spectra of the CNF specimens, which indicated that the end product was free of hemicellulose. In addition, the increase in absorbance at 898 cm^{-1} that corresponded to the C-H glycosidic deformation of cellulose (He *et al*. 2014) was consistent with increasing cellulosic content. Based on FTIR spectroscopic analysis, only the hydrothermal and xylanase treatments of kenaf bark and lignin were found to completely remove hemicellulose. Therefore, the bleaching process was necessary to facilitate complete lignin removal and increase CNF purity.

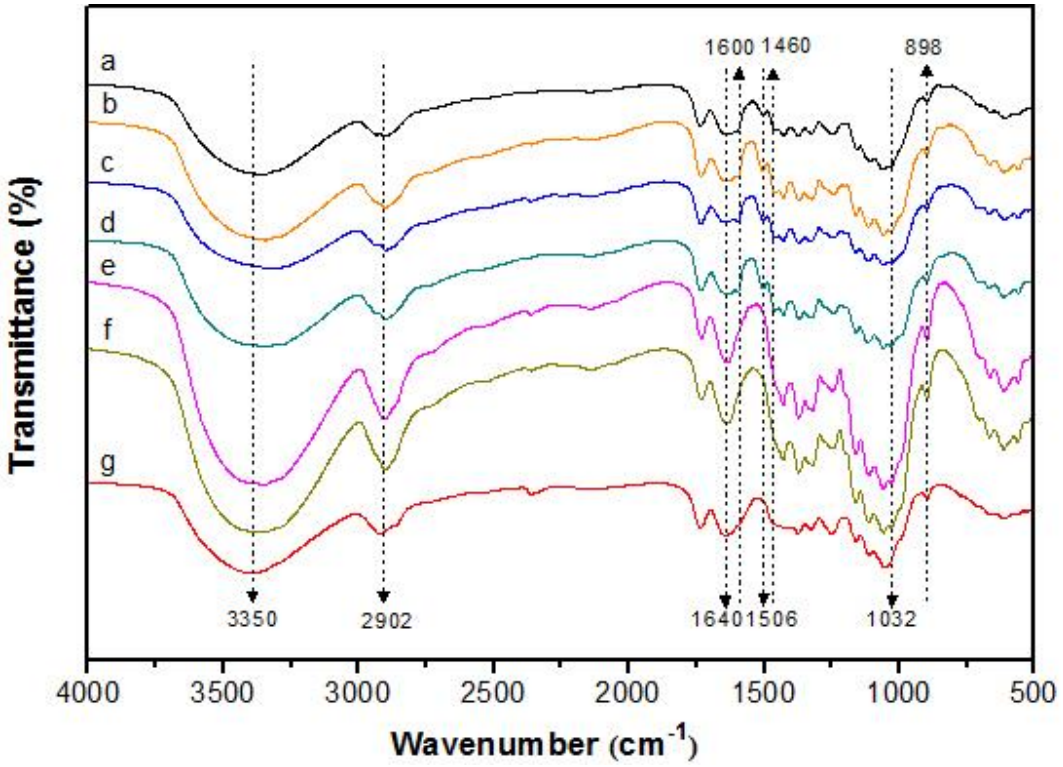

Fig. 7. FTIR spectra of (a) KB, (b) HT-KF, (c) HT-KF-NaAc buffer, (d) HT-KF-x5000, (e) HT-KF-NaAc buffer-B, (f) HT-KF-x5000-B, and (g) CNF

XRD Analysis

The X-ray diffraction patterns of the different fibers, including CNF, were analyzed as shown in Fig. 8. All samples showed reflection peaks typical of cellulose I at 2θ = 16°, 22°, and 34° (Xu *et al*. 2015). Thus, the mechano-enzymatic treatment applied to obtain CNF from KB did not change the structure of the cellulose crystal, as previously reported by Saelee *et al*. (2016), Tibolla *et al*. (2017), and Xu *et al*. (2015). A transformation from cellulose I to II was also reported to occur when using some chemical treatments (Miao *et al.* 2016). The reflection peak at 2θ = 22.56° became more intense after fiber treatment. The crystallinity index (CrI) of the sample continued to increase (Table 2) after hydrothermal treatment, xylanase treatment, and bleaching. The CrI of KB was 74.0% and it increased to 82.5% after hydrothermal treatment. After xylanase treatment, the CrI of HT-KF-x5000 fibers increased slightly to 83.8%. Comparable observations for other fibers in pulp form showed that the xylanase treatment increased the crystallinity of eucalyptus kraft pulp (Roncero *et al*. 2005), aspen pulp (Liu *et al*. 2012) and bagasse pulp (Saelee *et al*. 2016). Therefore, the impurities in the sample were successfully removed by the bleaching process, which consequently increased the CrI value.

However, the CrI of CNF after microfluidization dramatically decreased from 87.2% to 65.6% due to the destruction of the crystallinity of kenaf fibers under continuous shearing force generated by the microfluidics. This result was in good accordance with a previous work that reported some damage to the crystalline domain and a decrease in the CrI of CNF upon microfluidization (Saelee *et al*. 2016). In addition to microfluidization, the mechanical isolation of fibers using high-pressure homogenization and ultrasonication was also reported to reduce the crystallinity of the extracted CNF (Tonoli *et al*. 2012; Fatah *et al*. 2014; Xie *et al*. 2016). For the application of CNF as a filler in polymer, although the

crystallinity of the CNF declined, which led to a lower stiffness, the high ductility of CNF remained and could improve the ductility of the polymeric matrices (Tonoli *et al*. 2012).

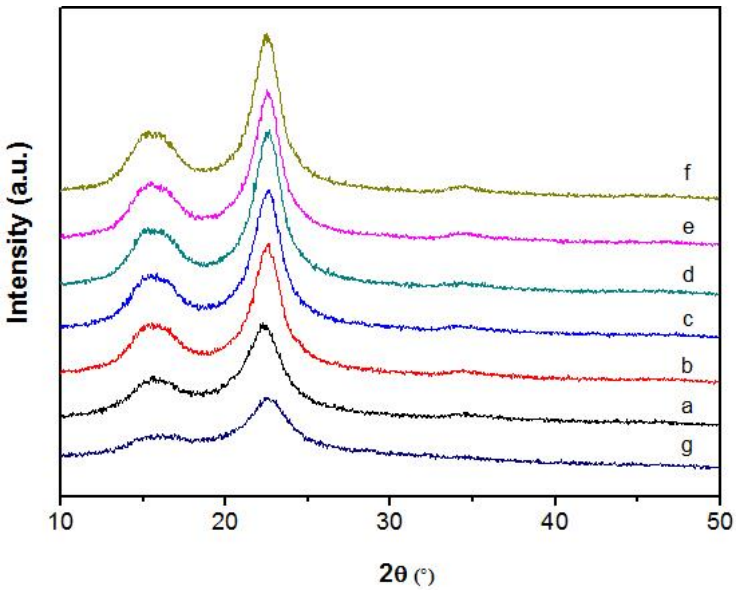

Fig. 8. X-ray diffraction patterns of (a) KB, (b) HT-KF, (c) HT-KF-NaAc buffer, (d) HT-KF-x5000, (e) HT-KF-NaAc buffer-B, (f) HT-KF-x5000-B, and (g) CNF

TGA of Kenaf Fiber

CNF has been used in biocomposite materials, which are processed at elevated temperatures of approximately 200 °C or above (Bandyopadhyay-Ghosh *et al*. 2010; Karimi *et al*. 2014). Therefore, the thermal properties of CNF analyzed by TG analysis and expressed as weight loss and derivative weight loss results were important. As shown in Fig. 9, all of the TG curves showed three thermal decomposition stages in the samples, indicating the presence of different components, cellulose, hemicellulose, and lignins, which usually decompose at different temperatures. The decomposition of hemicellulose started at 220 to 300 °C, before the breakdown of cellulose and lignin. The presence of acetyl groups in hemicellulose is responsible for its initial mass losses at these relatively low temperatures (He *et al*. 2014; Khawas and Deka 2016). The decomposition of cellulose started at 310 °C and ended at a temperature of approximately 400 °C (Xu *et al*. 2015). Lignins degrade in a very broad temperature range starting at 200 °C and ending at 700 °C (Abraham *et al*. 2013).

All samples showed a mass loss of approximately 5% in the temperature range of 30 to 100 °C, which was based on the loss of moisture (Fig. 9). In this temperature region, the vaporization and removal of unbound water in the cellulose begins (Chandra *et al*. 2016). The temperature of the start of degradation (T_{on}) and the temperature at maximum degradation (T_{max}) of all samples are summarized in Table 2. The decomposition of KB occurred at approximately 293.9 °C (13.2% mass loss), and T_{max} was 336.0 °C (57.4% mass loss). After hydrothermal treatment of the kenaf bark (HT-KF), the T_{on} and T_{max} were highly increased to 333.9 °C (7.41% mass loss) and 364.3 °C (70.5% mass loss), respectively. The T_{on} and T_{max} were higher than in the KB fibers, indicating the enhancement of thermal stability, which was directly related to the increase in the amount of cellulose in the sample. This finding also indicated that the hydrothermal treatment was able to effectively remove hemicellulose and part of the lignin.

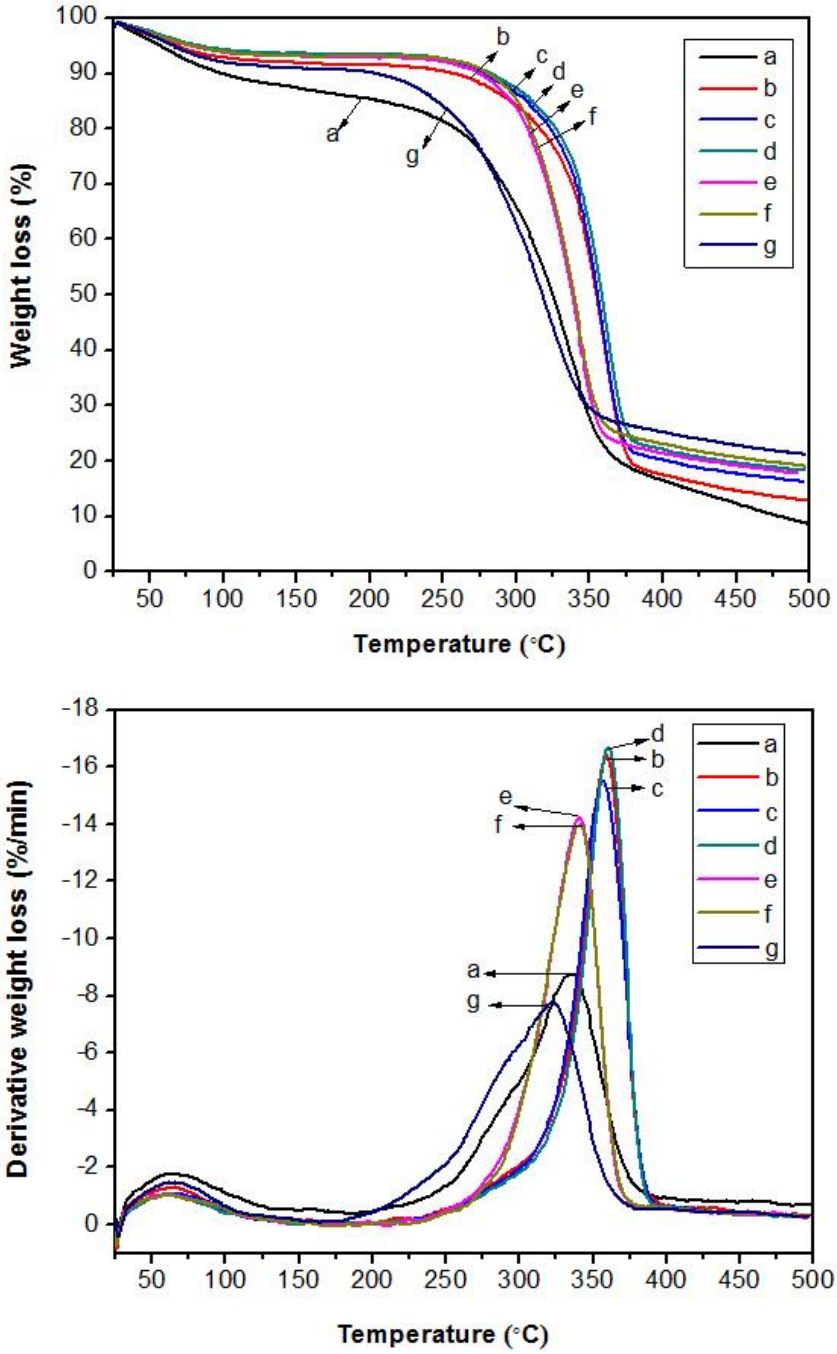

Fig. 9. TGA and DTG curves of (a) KB, (b) HT-KF, (c) HT-KF-NaAc buffer, (d) HT-KF-x5000, (e) HT-KF-NaAc buffer-B, (f) HT-KF-x5000-B, and (g) CNF

After xylanase treatment, the thermal stability curve of HT-KF-X5000 fibers (T_{on} = 336.6 °C, 5.57% mass loss and T_{max} = 365.0 °C, 70.9% mass loss) was considerably above the curve of the control sample (HT-KF NaAc buffer fibers). The xylanase treatment removed most of the hemicellulose from the sample and thus increased the thermal stability of the specimen. However, the thermal stability of the bleached fiber samples (HT-KF-NaAc buffer-B and HT-KF-x5000-B) was lower than that of the unbleached samples (HT-KF-X5000 and HT-KF-NaAc buffer fibers). The hypothesis was that this change resulted

from the bleaching process in acidic conditions, which affected the delignification of the sample. Therefore, the molecular structure of cellulose was slightly changed or more open due to the removal of the aromatic ring of lignin penetrating into the cellulose molecule (Saelee *et al*. 2016). The molecular structure of cellulose was also assumed to be looser after the bleaching process than in the unbleached sample, which allowed a higher contact area and lower thermal stability.

In the case of CNF thermal stability, the T_{on} measured for the CNF specimen was 271.7 °C with a mass loss of 8.08% and the T_{max} was 321.6 °C with a mass loss of 61.8%. These data showed that the thermal stability of the CNF was substantially lower than that of the bleached samples and similar to that of untreated kenaf bark (KB). The lower thermal stability of the CNF was mainly due to the small size of the CNF, which allowed for the exposure of a higher surface area to external conditions. Smaller particles can be more easily degraded and are less heat resistant because of their higher surface area/volume ratio (Quiévy *et al*. 2010; Zhao *et al*. 2013).

The percentages of remaining fiber dregs after the samples were heated to 500 °C in an inert atmosphere are summarized in Table 2. The CNF showed the highest amount of carbonized substance. This result was explained by the formation of anhydrocellulose related to dehydration reactions combined with a subsequent decomposition of the anhydrocellulose to carbonaceous residues or biochar (Quiévy *et al*. 2010; Jacquet *et al*. 2011).

Table 2. Crystallinity Index (CrI) and Thermal Properties of the Fibers After the Different Stages of Treatment

Fibers	Crystallinity Index (% CrI)	T_{on} (ºC)	Mass Loss (%)	T_{max} (ºC)	Mass Loss (%)	Residue at 500 ºC (%)
KB	73.99	293.94	13.15	336.01	57.44	8.57
HT-KF	82.46	333.94	7.41	364.27	70.47	12.85
HT-KF-NaAc buffer	83.35	335.22	6.15	361.66	71.57	16.24
HT-KF-x5000	83.81	336.64	5.57	365.02	70.87	18.23
HT-KF-NaAc buffer -B	84.83	312.01	6.01	344.95	71.07	17.63
HT-KF-x5000-B	87.19	311.88	6.06	345.16	69.95	19.05
CNF	65.60	271.96	8.08	321.58	61.81	21.17

CONCLUSIONS

1. The hydrothermal, xylanase, and bleaching treatment of the kenaf bark led to effective cellulose purification, and the cellulose content and whiteness index of the fiber selected for CNF isolation were 85.1% and 85.9, respectively.
2. The results of the FTIR, XRD, and TG analyses confirmed that the removal of hemicellulose and lignin were affected by the mechano-enzymatic treatment.
3. The CNF was successfully isolated from the kenaf bark *via* combined mechanical and enzymatic treatments. Web-like CNF structures were 5 to 10 nm in diameter with lengths in the micrometer range and no undesired elemental contamination.

4. The CNF from the experiment was high in purity, had a good appearance, and showed promising mechanical and thermal properties. It was suitable for various applications, such as biomedical uses and advanced material processing.
5. The proposed mechano-enzymatic treatment of kenaf bark for CNF production was a clean and environmentally friendly process that led to lower consumption of chemicals used in the bleaching and overall process.

ACKNOWLEDGMENTS

The authors are grateful for the financial support of this research from the National Research Council of Thailand (NRCT) and the Research Promotion and Technology Transfer Center (RPTTC), Faculty of Liberal Arts and Science, Kasetsart University, Thailand. Moreover, the authors are thankful to the Enzyme Technology Laboratory, Microbial Biotechnology and Biochemicals Research Unit, and the National Center for Genetic Engineering and Biotechnology (BIOTEC), Thailand for providing equipment and instruments.

REFERENCES CITED

Abdul Khalil, H. P. S., Davoudpour, Y., Saurabh, C. K., Hossain, M. S., Adnan, A. S., Dungani, R., Paridah, M. T., IslamSarker, M. Z., Nurul Fazita, M. R., Syakir, M. I., *et al*. (2016). "A review on nanocellulosic fibres as new material for sustainable packaging: Process and applications," *Renew. Sust. Energ. Rev.* 64, 823-836. DOI: 10.1016/j.rser.2016.06.072

Abraham, E., Deepa, B., Pothen, L. A., Cintil, J., Thomas, S., John, M. J., Anandjiwala, R., and Narine, S. S. (2013). "Environmentally friendly method for the extraction of coir fibre and isolation of nanofibre," *Carbohyd. Polym*. 92(2), 1477-1483. DOI: 10.1016/j.carbpol.2012.10.056

Agbor, V. B., Cicek, N., Sparling, R., Berlin, A., and Levin, D. B. (2011). "Biomass pretreatment: Fundamentals toward application," *Biotechnol. Adv*. 29(6), 675-685. DOI: 10.1016/j.biotechadv.2011.05.005

Alemdar, A., and Sain, M. (2008). "Biocomposites from wheat straw nanofibers: Morphology, thermal and mechanical properties," *Compos. Sci. Technol*. 68(2), 557-565. DOI: 10.1016/j.compscitech.2007.05.044

Alvira, P., Tomás-Pejó, E., Ballesteros, M., and Negro, M. J. (2010). "Pretreatment technologies for an efficient bioethanol production process based on enzymatic hydrolysis: A review," *Bioresource Technol*. 101(13), 4851-4861. DOI: 10.1016/j.biortech.2009.11.093

Bandyopadhyay-Ghosh, S., Bandhu Ghosh, S., and Sain, M. (2010). "Cellulose nanocomposites," in: *Industrial Applications of Natural Fibres - Structure, Properties and Technical Applications*, J. Müssig (ed.), John Wiley & Sons, Ltd., Chichester, UK, pp. 459-480.

Chandra, J. C. S., George, N., and Narayanankutty, S. K. (2016). "Isolation and characterization of cellulose nanofibrils from arecanut husk fibre," *Carbohyd. Polym.* 142, 158-166. DOI: 10.1016/j.carbpol.2016.01.015

Fan, S., Zhang, P., Li, F., Jin, S., Wang, S., and Zhou, S. (2016). "A review of lignocellulose change during hydrothermal pretreatment for bioenergy production," *Curr. Org. Chem.* 20, 1-11. DOI: 10.2174/1385272820666160513154 113

Fatah, I. Y. A., Abdul Khali, H. P. S., Hossain, M. S., Aziz, A. A., Davoudpour, Y., Dungani, R., and Bhat, A. (2014). "Exploration of a chemo-mechanical technique for the isolation of nanofibrillated cellulosic fiber from oil palm empty fruit bunch as a reinforcing agent in composites materials," *Polymers* 6(10), 2611-2624. DOI: 10.3390/polym6102611

Gan, S., Zakaria, S., Chia, C. H., Padzil, F. N. M., and Ng, P. (2015). "Effect of hydrothermal pretreatment on solubility and formation of kenaf cellulose membrane and hydrogel," *Carbohyd. Polym.* 115, 62-68. DOI: 10.1016/j.carbpol.2014.08.093

Gangwar, A. K., Prakash, N. T., and Prakash, R. (2016). "An eco-friendly approach: Incorporating a xylanase stage at various places in ECF and chlorine-based bleaching of eucalyptus pulp," *BioResources* 11(2), 5381-5388. DOI: 10.15376/biores.11.2.5381-5388

Ghanbarzadeh, B., Almasi, H., and Entezami, A. A. (2010). "Physical properties of edible modified starch/carboxymethyl cellulose films," *Innov. Food Sci. Emerg.* 11(4), 697-702. DOI: 10.1016/j.ifset.2010.06.001

Hassan, M. L., Bras, J., Hassan, E. A., Silard, C., and Mauret, E. (2014). "Enzyme-assisted isolation of microfibrillated cellulose from date palm fruit stalks," *Ind. Crop. Prod.* 55, 102-108. DOI: 10.1016/j.indcrop.2014.01.055

He, W., Xiaochuan, J., Fengwen, S., and Xinwu, X. (2014). "Extraction and characterization of cellulose nanofibers from *Phyllostachys nidularia* Munro *via* a combination of acid treatment and ultrasonication," *BioResources* 9(4), 6876-6887. DOI: 10.15376/biores.9.4.6876-6887

Henriksson, M., Henriksson, G., Berglund, L. A., and Lindström, T. (2007). "An environmentally friendly method for enzyme-assisted preparation of microfibrillated cellulose (MFC) nanofibers," *Eur. Polym. J.* 43(8), 3434-3441. DOI: 10.1016/j.eurpolymj.2007.05.038

Jacquet, N., Quiévy, N., Vanderghem, C. Janas, S., Blecker, C., Wathelet, B., Devaux, J., and Paquot, M. (2011). "Influence of steam explosion on the thermal stability of cellulose fibres," *Polym. Degrad. Stabil.* 96(9), 1582-1588. DOI: 10.1016/j.polymdegradstab.2011.05.021

Janardhnan, S., and Sain, M. (2011). "Bio-treatment of natural fibers in isolation of cellulose nanofibres: Impact of pre-refining of fibers on treatment efficiency and nanofiber yield," *J. Polym. Environ.* 19(3), 615-621. DOI: 10.1007/s10924-011-0312-6

Jonoobi, M., Harun, J., Shakeri, A., Misra, M., and Oksman, K. (2009). "Chemical composition, crystallinity and thermal degradation of bleached and unbleached kenaf bast (*Hibiscus cannabinus*) pulp and nanofibers," *BioResources* 4(2), 626-639. DOI: 10.15376/biores.4.2.626-639

Kalia, S., Thakur, K., Celli, A., Kiecheland, M. A., and Schauer, C. L. (2013). "Surface modification of plant fibers using environment friendly methods for their application in polymer composites, textile industry and antimicrobial activities: A review," *J. Environ. Chem. Eng.* 1(3), 97-112. DOI: 10.1016/j.jece.2013.04.009

Karimi, S., Tahir, P. M., Dufresne, A., Karimiand, A., and Abdulkhani, A. (2014). "Kenaf bast cellulosic fibers hierarchy: A comprehensive approach from micro to nano," *Carbohyd. Polym.* 101, 878-885. DOI: 10.1016/j.carbpol.2013.09.106

Kaushik, A., and Singh, M. (2011). "Isolation and characterization of cellulose nanofibrils from wheat straw using steam explosion coupled with high shear homogenization," *Carbohyd. Res*. 346(1), 76-85. DOI: 10.1016/j.carres.2010.10.020

Khawas, P., and Deka, S. C. (2016). "Isolation and characterization of cellulose nanofibers from culinary banana peel using high-intensity ultrasonication combined with chemical treatment," *Carbohyd. Polym*. 137, 608-616. DOI: 10.1016/j.carbpol.2015.11.020

Kumar, R., Hu, F., Hubbell, C. A., Ragauskas, A. J., and Wyman, C. E. (2013). "Comparison of laboratory delignification methods, their selectivity, and impacts on physiochemical characteristics of cellulosic biomass," *Bioresource Technol*. 130, 372-381. DOI: 10.1016/j.biortech.2012.12.028

Li, M., Wang, L.-J., Li, D., Cheng, Y.-L., and Adhikari, B. (2014). "Preparation and characterization of cellulose nanofibers from de-pectinated sugar beet pulp," *Carbohyd. Polym*. 102(1), 136-143. DOI: 10.1016/j.carbpol.2013.11.021

Liang, L., Huang, C., and Ragauskas, A. J. (2017). "Nanocellulose-based materials for biomedical applications," *JSM Chemistry* 5(3), 1048-1050.

Lin, N., and Dufresne, A. (2014). "Nanocellulose in biomedicine: Current status and future prospect," *Eur. Polym. J*. 59, 302-325. DOI: 10.1016/j.eurpolymj.2014.07.025

Liu, N., Qin, M., Gao, Y., Li, Z., Fu, Y., and Xu, Q. (2012). "Pulp properties and fiber characteristics of xylanase-treated aspen APMP," *BioResources* 7(3), 3367-3377. DOI: 10.15376/biores.7.3.3367-3377

Liu, Q., Lu, Y., Aguedo, M., Jacquet, N., Ouyang, C., He, W., Yan, C., Bai, W., Guo, R., Goffin, D., *et al.* (2017). "Isolation of high-purity cellulose nanofibers from wheat straw through the combined environmentally friendly methods of steam explosion, microwave-assisted hydrolysis, and microfluidization," *ACS Sustain. Chem. Eng*. 5(7), 6183-6191. DOI: 10.1021/acssuschemeng.7b01108

Ma, X. J., Cao, S. L., Lin, L., Luo, X. L., Hu, H. C., Chen, L. H., and Huang, L. L. (2013). "Hydrothermal pretreatment of bamboo and cellulose degradation," *Bioresource Technol.* 148, 408-413. DOI: 10.1016/j.biortech.2013.09.021

Marrakchi, Z., Khiari, R., Queslati, H., Mauret, E., and Mhenni, F. (2011). "Pulping and papermaking properties of Tunisian alfa stems (*Stipa tenacissima*) - Effects of refining process," *Ind. Crop. Prod*. 34(3), 1572-1582. DOI: 10.1016/j.indcrop.2011.05.022

Martelli-Tosi, M., Torriccillas, M. S., Martins, M. A., Assis, O. B. G., and Tapia-Blácido, D. R. (2016). "Using commercial enzymes to produce cellulose nanofibers from soybean straw," *J. Nanomater*. 2016, 1-10. DOI: 10.1155/2016/8106814

Miao, X., Lin, J., Tian, F., Li, X., Bian, F., and Wang, J. (2016). "Cellulose nanofibrils extracted from the byproduct of cotton plant," *Carbohyd. Polym*. 136, 841-850. DOI: 10.1016/j.carbpol.2015.09.056

Miller, G. L. (1959). "Use of dinitrosalicylic acid reagent for determination of reducing sugar," *Anal. Chem*. 31(3), 426-428. DOI: 10.1021/ac60147a030

Oun, A. A., and Rhim, J. W. (2016). "Characterization of nanocelluloses isolated from Ushar (*Calotropis procera*) seed fiber: Effect of isolation method," *Mater. Lett*. 168, 146-150. DOI: 10.1016/j.matlet.2016.01.052

Patel, B., Guo, M., Izadpanah, A., Shah, N., and Hellgardt, K. (2016). "A review on hydrothermal pre-treatment technologies and environmental profiles of algal biomass processing," *Bioresource Technol.* 199, 288-299. DOI: 10.1016/j.biortech.2015.09.064

Pei, Y., Wang, S., Qin, C., Su, J., Nie, S., and Song, X. (2016). "Optimization laccase-aided chlorine dioxide bleaching of bagasse pulp," *BioResources* 11(1), 696-712. DOI: 10.15376/biores.11.1.696-712

Quiévy, N., Jacquet, N., Sclavons, M., Deroanne, C., Paquot, M., and Devaux, J. (2010). "Influence of homogenization and drying on the thermal stability of microfibrillated cellulose," *Polym. Degrad. Stabil.* 95(3), 306-314. DOI: 10.1016/j.polymdegradstab.2009.11.020

Rahimi Kord Sofla, M., Brown, R. J., Tsuzuku, T., and Rainey, T. J. (2016). "A comparison of cellulose nanocrystals and cellulose nanofibers extracted from bagasse using acid and ball milling methods," *Adv. Nat. Sci.- Nanosci.* 7(3), 1-9. DOI: 10.1088/2043-6262/7/3/035004

Roncero, M. B., Torres, A. L., Colom, J. F., and Vidal, T. (2005). "The effect of xylanase on lignocellulosic components during the bleaching of wood pulps," *Bioresource Technol*. 96(1), 21-30. DOI: 10.1016/j.biortech.2004.03.003

Sabo, R., Yermakov, A., Law, C. T., and Elhajjar, R. (2016). "Nanocellulose-enabled electronics, energy harvesting devices, smart materials and sensors: A review," *J. Renew. Mater.* 4(5), 297-312. DOI: 10.7569/JRM.2016.634114

Saelee, K., Yingkamhaeng, N., Nimchua, T., and Sukyai, P. (2016). "An environmentally friendly xylanase-assisted pretreatment for cellulose nanofibrils isolation from sugarcane bagasse by high-pressure homogenization," *Ind. Crop. Prod.* 82, 149-160. DOI: 10.1016/j.indcrop.2015.11.064

Segal, L., Creely, J. J., Martin, A. E., and Conrad, C. M. (1959). "An empirical method for estimating the degree of crystallinity of native cellulose using the X-ray diffractometer," *Text. Res. J.* 29(10), 786-794. DOI: 10.1177/004051755902901003

Shatalov, A. A., and Pereira, H. (2009). "Impact of hexenuronic acids on xylanase-aided bio-bleaching of chemical pulps," *Bioresource Technol.* 100(12), 3069-3075. DOI: 10.1016/j.biortech.2009.01.020

Siddiqui, N., Mills, R. H., Gardner, D. J., and Bousfield, D. (2010). "Production and characterization of cellulose nanofibers from wood pulp," *J. Adhes. Sci. Technol*. 25(6-7), 709-721. DOI: 10.1163/016942410X525975

Sulaiman, S., Mokhtar, M. N., Naim, M. N., Baharuddin, A. S., Salleh, M. A. M., and Sulaiman, A. (2015). "Study on the preparation of cellulose nanofibre (CNF) from kenaf bast fibre for enzyme immobilization application," *Sains Malays*. 44(11), 1541-1550.

Tibolla, H., Pelissari, F. M., Rodrigues, M. I., and Menegalli, F. C. (2017). "Cellulose nanofibers produced from banana peel by enzymatic treatment: Study of process conditions," *Ind. Crop. Prod*. 95, 664-674. DOI: 10.1016/j.indcrop.2016.11.035

Tonoli, G. H. D., Teixeira, E. M., Corrêa, A. C., Marconcini, J. M., Caixeta, L. A., Pereira-da-Silva, M. A., and Mattoso, L. H. C. (2012). "Cellulose micro/nanofibres from *Eucalyptus* kraft pulp: Preparation and properties," *Carbohyd. Polym*. 89(1), 80-88. DOI: 10.1016/j.carbpol.2012.02.052

Van Soest, P. J. (1963). "Use detergents in the analysis of fibrous feeds II. A rapid method for the determination of fiber and lignin," *J. Assoc. Off. Ana. Chem*. 46(5), 829-835.

Xiao, L. P., Sun, Z. J., Shi, Z. J., Xu, F., and Sun, R. C. (2011). "Impact of hot compressed water pretreatment on the structural changes of woody biomass for bioethanol production," *BioResources* 6(2), 1576-1598 DOI: 10.15376/biores.6.2.1576-1598

Xie, J., Hse, C.-Y., De Hoop, C. F., Hu, T., Qi, J., and Shupe, T. F. (2016). "Isolation and characterization of cellulose nanofibers from bamboo using microwave liquefaction combined with chemical treatment and ultrasonication," *Carbohyd. Polym*. 151, 725-734. DOI: 10.1016/j.carbpol.2016.06.011

Xu, C., Zhu, S., Xing, C., Li, D., Zhu, N., and Zhou, H. (2015). "Isolation and properties of cellulose nanofibrils from *coconut palm petioles* by different mechanical process," *PLOS One* 10(4), 1-11 DOI: 10.1371/journal.pone.0122123

Zhang, X., Han, G., Jiang, W., Zhang, Y., Li, X., and Li, M. (2016). "Effect of steam pressure on chemical and structural properties of kenaf fibers during steam explosion process," *BioResources* 11(3), 6590-6599. DOI: 10.15376/biores.11.3.6590-6599

Zhao, J., Zhang, W., Zhang, X., Zhang, X., Lu, C., and Deng, Y. (2013). "Extraction of cellulose nanofibrils from dry softwood pulp using high shear homogenization," *Carbohyd. Polym.* 97(2), 695-792. DOI: 10.1016/j.carbpol.2013.05.050

Article submitted: August 10, 2018; Peer review completed: October 28, 2018; Revised version received and accepted: November 2, 2018; Published: November 9, 2018.
DOI: 10.15376/biores.14.1.99-119